Using lignocellulosic fractions of coffee husk to improve properties of compatibilised starch-PLA blend films

Sofía Collazo-Bigliardi[a*], Rodrigo Ortega-Toro[b] and Amparo Chiralt[a]

[a]Instituto de Ingeniería de Alimentos para el Desarrollo, Universidad Politécnica de Valencia, Camino de Vera s/n, 46022 Valencia, Spain. socol@alumni.upv.es; dchiralt@tal.upv.es

[b]Programa de Ingeniería de Alimentos, Facultad de Ingeniería, Universidad de Cartagena, Carrera 6 # 36-100, Cartagena de Indias D.T y C, Colombia. rortegap1@unicartagena.edu.co

*Corresponding author: Sofía Collazo-Bigliardi. Instituto de Ingeniería de Alimentos para el Desarrollo, Universidad Politécnica de Valencia, Camino de Vera s/n, 46022 Valencia, Spain. Phone: 34-963877924. Fax: 34-963877926. socol@alumni.upv.es

ABSTRACT

The effectiveness of the incorporation of cellulosic reinforcing agents (cellulosic fibres: CF and cellulose nanocrystals: CNC) and antioxidant aqueous extract (AE) from coffee husk at improving the functional properties of compatibilised starch-PLA blend films was studied. Tensile and barrier properties, crystallization pattern and thermal behaviour were analysed in films containing 1wt% of CF or CNC incorporated by two different methods or 5.8 wt% of antioxidant extract. The antioxidant properties of the films were also tested through their efficacy at preserving sunflower oil from oxidation. Of the cellulosic fractions, CNC directly blended with the starch phase were the most effective

at reinforcing tensile properties of the material (148% and 45% increase in elastic modulus and tensile strength, respectively) and at reducing their water vapour and oxygen permeability (28% and 42% reduction, respectively). The AE did not improve the mechanical performance of the blend films, but conferred antioxidant capacity useful for food packaging applications.

Keywords: Coffee husk; Cellulose fillers; Antioxidant extracts; Starch; Polylactic acid; Grafted polycaprolactone.

1. Introduction

Nowadays, it is a challenge to develop materials able to substitute the conventional petroleum-derived polymers with high environmental impact due to their accumulation and difficult management (Balaji, Pakalapati, Khalid, Walvekar, & Siddiqui, 2017). This is especially convenient in the food packaging area where there is a very high consumption of plastic materials. In this sense, biodegradable materials should substitute synthetic plastics since they represent an attractive solution to this issue, being abundant and mostly obtained from renewable resources. Different groups of biodegradable polymers have been studied, such as those directly obtained from biomass (polysaccharides, proteins and those produced by microbial action) and those synthesised from bio-based monomers (polylactic acid: PLA) or from petrochemical products (poly (ε-caprolactone): PCL) (Brigham, 2018; Collazo-Bigliardi, Ortega-Toro, & Chiralt, 2018a). These materials can also be used in combination, forming multilayer packaging systems (Requena, Vargas, & Chiralt, 2018; Tampau, González-Martínez, & Chiralt, 2018) or composites (Ortega-Toro, Collazo-Bigliardi, Talens, & Chiralt, 2016a) with optimized mechanical and barrier properties for food packaging.

Starch and PLA are the most widely-studied biomaterials for food packaging applications. Starch from different sources (rice, potato, corn, cassava, wheat, etc.) can be transformed into thermoplastic starch (TPS) by thermo-mechanical treatment in combination with the action of plasticizers (Koch, 2018). Despite its hydrophilic nature and water sensitivity, its limited mechanical performance and retrogradation during storage, starch is an interesting polymer for food packaging development due to its suitability for food contact, competitive price and high oxygen barrier capacity (Ortega-Toro, Bonilla, Talens, & Chiralt, 2017). Likewise, starch modification through the reaction of hydroxyl groups (-OH) provides several possibilities for modulating its properties (Ogunsona, Ojogbo, & Mekonnen, 2018). As concerns PLA, it is synthesized from lactic acid obtained in the dextrose fermentation, using renewable sources, such as corn starch, rice starch or raw materials with high sugar content. This biodegradable aliphatic polyester is commonly produced by the ring-opening polymerization (ROP) of lactide monomers formed from lactic acid (Balaji et al., 2017; Muller, González-Martínez, & Chiralt, 2017a). PLA is easy to process, transparent and has excellent water vapour barrier permeability (Murariu & Dubois, 2016), with characteristics comparable to those traditional petrochemical-based polymers (such as polystyrene: PS or polyethylene terephthalate: PET). However, PLA exhibits low oxygen barrier capacity in line with its hydrophobic nature and limited toughness, despite the fact that it is resistant to traction (Hamad, Kaseem, Ayyoob, Joo, & Deri, 2018).

TPS-PLA blends have been studied to make the most of their complementary properties for the purposes of designing packaging materials. Nevertheless, these polymers are not thermodynamically compatible and their blends exhibit phase separation, which limits their effectiveness (Müller et al., 2016). Then, it is necessary to improve their interfacial adhesion in order to obtain TPS-PLA blends with better functional properties. To this

end, the use of compatibilizers has been widely studied (Hamad et al., 2018). Different compounds, such as citric acid, stearic acid, maleic anhydride, dicumyl peroxide or citrate esters, have been used to enhance the mechanical, thermal and barrier properties of the blends (Muller et al., 2017a). Ortega-Toro et al. (2016b) studied the use of compatibilizers based on the melt grafting of poly(ε-caprolactone) (PCL) with reactive polar groups from glycidyl methacrylate (epoxide) or maleic anhydride (anhydride), as reported by Laurienzo, Malinconico, Mattia and Romano (2006), in TPS-PCL blends. These compatibilizers have also been used in TPS-PLA blends leading to films with improved functional properties (Collazo-Bigliardi, Ortega-Toro & Chiralt, 2019a). Particularly, films with 20% substitution of starch by PLA, containing 5% of grafted PCL with glycidyl methacrylate exhibited high resistance to break and reduced water vapour permeability with respect to the starch films, with very high oxygen barrier capacity. The incorporation of cellulosic fibres and antioxidant compounds into this matrix might still improve the film characteristics for their application in food packaging.

Micro- or nano-fillers from different sources have been studied to improve the functional properties of biopolymer films (Collazo-Bigliardi et al., 2018a). In particular, lignocellulosic agro-wastes have been commonly used to isolate microcrystalline cellulose and cellulose nanocrystals. These fillers have been incorporated into starch-based blends (Azeredo, Rosa, & Mattoso, 2017; Berthet et al., 2015; Collazo-Bigliardi, Ortega-Toro, & Chiralt, 2018b; Patel & Parsania, 2017) and provided great thermal resistance, improving the elastic modulus and barrier properties of composites. The presence of the hydroxyl groups of the cellulose favours its interaction with the polymer matrix, thus contributing to its reinforcement.

Lignocellulosic materials are also a source of phenolic compounds, which exhibit active properties to control microbial or oxidative processes in food matrices (Cong-Cong, Bing, Yi-Qiong, Jian-Sheng, & Tong; Shavandi et al., 2018). The antioxidant character of polyphenols is related with their ability both to act as free radical scavengers, inhibiting lipoxygenase enzyme activity, and to chelate metals (Talón, Trifkovic, Vargas, Chiralt, & González-Martínez, 2017).

In this context, coffee husk (endocarp of coffee beans) is an interesting raw material produced in coffee processing, with high content of both cellulosic (35%, Collazo-Bigliardi et al., 2018b) and phenolic components (1.3 % in Gallic Acid Equivalents, Collazo-Bigliardi et al., 2019b) that can be valued through its use for packaging material development (Alves, Rodrigues, Nunes, Vinha, & Oliveira, 2017). This residue has been submitted to hydrothermal treatments to extract active compounds (Piñeros-Castro & Otálvaro, 2014), and to different chemical treatments in order to isolate cellulose fibres, whose subsequent acid hydrolysis produced cellulose nanocrystals. The isolated CNC exhibited an aspect ratio ranging between 20-40, which confers good reinforcing properties, 92% crystallinity and high thermal resistance (Collazo-Bigliardi et al., 2018b).

The aim of this work was to analyse the effectiveness of the incorporation of cellulosic reinforcing agents (cellulose fibres and cellulose nanocrystals) and antioxidant aqueous extract from coffee husk at improving the functional properties of compatibilized starch-PLA blend films. The antioxidant properties of the films were tested through their efficacy at preserving sunflower oil from oxidation. The effect of the incorporation method of cellulose nanocrystals into the blend films was also analysed.

2. Materials and methods

125 *2.1. Materials*

126 Corn starch (S, 28% amylose) was supplied by Roquette (Roquette Laisa, Benifaió,
127 Spain) and amorphous PLA 4060D, density of 1.24 g/cm^3, was purchased from
128 Natureworks (U.S.A). Glycerol was obtained from Panreac Química, S.A. (Castellar del
129 Vallès, Barcelona, Spain). For the chemical modification of PCL (pellets ~3 mm,
130 average Mn 80.000 Da), glycidyl methacrylate (G) (purity 97%) and benzoyl peroxide
131 (BP) were supplied by Sigma (Sigma-Aldrich Chemie, Steinheim, Germany). Coffee
132 husks were provided by Universidad Jorge Tadeo Lozano (Bogotá, Colombia) and
133 maltodextrin 18 DE used in spray drying of extracts was from Tecnas S.A., Colombia.

134

135 *2.2. Preparation of grafted PCL*

136 The grafting reaction of glycidyl methacrylate (G) to PCL was performed following the
137 methodology described by Collazo-Bigliardi et al. (2019a), Ortega-Toro et al. (2016b)
138 and Laurienzo et al. (2006). To this end, 45 g of PCL, 0.5 g of BP and 5 g of G were
139 incorporated into the Brabender plastograph (EC Plus, Duisburg, Germany) and melt
140 blended at 100 ºC and 32 rpm for 20 min to obtain PCL_G. Modified PCL_G was dissolved
141 in 500 mL of chloroform, subsequently re-precipitated in excess of hexane for the
142 purposes of removing any ungrafted reagents (oligomers and monomers residuals), and
143 kept in a desiccator under vacuum for 12 h at 25 ºC, and stored under freezing till its
144 use. The molar grafting ratio determined for the glycidyl methacrylate in PCL_G was 4.3
145 ± 0.4%, determined from H^1 NMR in previous studies (Collazo-Bigliardi et al., 2019a;
146 Ortega-Toro et al., 2016b).

147

148 *2.3. Extraction of antioxidant compound and isolation of cellulosic materials from*
149 *coffee husk*

150 The extraction of the antioxidant fraction was carried out with 650 g of coffee husk and
151 3 L of distilled water in a 5 L capacity pilot scale reactor (A2423 model, Amar
152 Equipment, India) by pressurised hot water (180 °C and 9.5 bar) for 60 min, according
153 to previous studies (Piñeros-Castro & Otálvaro, 2014). The extracts were separated
154 from the solid fraction which was dried for the purposes of subsequently extracting the
155 cellulose fillers. The extract was concentrated at 90 °C under continuous stirring and
156 then spray dried using a Vibrasec pilot dryer model Pasalab 1.5 (Universidad Nacional
157 de Colombia, Medellin), operating at 180 ºC and 90 ºC outlet temperature, at an
158 atomiser disk speed of 24,000 rpm. Maltodextrin (18 DE) at 29.8 wt% was added as
159 drying coadjuvant.
160 The process of isolating cellulose reinforcing agents from coffee husks was carried out
161 following the methodology reported by Collazo-Bigliardi et al. (2018b). The solid
162 residue from the hydrothermal treatment was alkali treated with 4 wt% of NaOH at 80
163 ºC for 3 h. Then, the sample was washed with distilled water until the alkali solution
164 was removed. The bleaching process to obtain cellulose fibres (CF) was completed by
165 adding equal parts of acetate buffer solution, sodium chlorite (1.7 wt%) and distilled
166 water to the alkali- treated solid at reflux temperature (~100 ºC) for 4 h, under
167 mechanical stirring. This process was repeated 4 times until the samples were
168 completely white. Then, the fibres were washed with distilled water several times, dried
169 and ground in a Moulinex grinder DJ200031 350W. Cellulose content of the isolated
170 fibres was 62±3% according to the previous study (Collazo-Bigliardi et al., 2018b).
171 Cellulose nanocrystals (CNC) were prepared by acid hydrolysis of the obtained
172 bleached fibres by 64% wt/wt sulphuric acid, at 50 °C for 40 min. The hydrolysed
173 sample was washed with distilled water by centrifugation at 14,000 rpm for 30 min.
174 Then, the suspension was dialysed against distilled water until constant pH and

neutralised with 10 wt% ion resin (Dowex Marathon MR-3) for 24 h. Finally, the CNC suspension was sonicated for 30 min using a tip sonicator (Vibra-Cell™ VCX 750, Sonics & Materials, Inc., Newton, USA) and kept refrigerated.

2.4. Obtaining compatibilised films

Films were obtained by melt blending the different components by using an internal mixer (HAAKE™ PolyLab™ QC, Thermo Fisher Scientific, Germany) at 160 °C and 50 rpm, for 10 min. The different film formulations and the mass ratio of the respective components are shown in Table 1. In all cases, 30 wt% of glycerol and 20 wt% of PLA with respect to starch were used and 5 wt%, with respect to the total polymer, of compatibiliser PCL_G. Cellulosic material (CF or CNC) was added at 1wt% and dry antioxidant extract (AE) was added at 5.8 wt%. The incorporation of 1 wt% of CNC into the films required specific previous steps, as commented on below. The obtained blends were cut into pellets and conditioned at 25 ºC and 53% relative humidity (RH) for one week before the film performance.

The films were obtained by compression moulding using a hot plate press (Model LP20, Labtech Engineering, Thailand). 4 g of the conditioned pellets were put onto Teflon sheets, preheated for 3 min at 160ºC and compression moulded for 1 min at 30 bars, followed by 3 min at 130 bars; thereafter, a 3 min cooling cycle was applied. Films were conditioned at 25 ºC and 53% RH for 1 week before their characterisation.

2.4.1. *The incorporation of CNC*

Since the obtained CNC were in aqueous dispersion (at 1 wt%) to prevent their aggregation (Brinchi, Cotana, Fortunati, & Kenny, 2013; Ng et al., 2015), their incorporation into the blend films required different strategies aimed at dispersing CNC

200 within the polymer matrix. Since no water could be included in the internal mixer used
201 for polymer melt blending to prevent overpressure, two different strategies were used:
202 method 1) the initial transference of CNC to the glycerol, following the method
203 described by Dorris & Gray (2012) and method 2) the prior thermoprocessing of the
204 aqueous dispersion of CNC containing glycerol and starch granules in a two-roll mill to
205 obtain CNC-TPS pellets.
206 In method 1 (M1), the aqueous CNC suspension after sonication was mixed with the
207 corresponding amount of glycerol under continuous stirring for 30 min (Dorris & Gray,
208 2012) and the water was subsequently removed by evaporation in an oven at 74ºC. The
209 CNC-glycerol blend, starch, PLA and PCL_G were melt blended in the internal mixer as
210 described above. In method 2 (M2), starch and glycerol were dispersed in the aqueous
211 CNC suspension and then thermoprocessed in a two-roll mill (Model LRM-M-100,
212 Labtech Engineering, Thailand roller) at 160 ºC for 15 min. The obtained pellets were
213 melt blended with PLA and PCL_G in the internal mixer under the same conditions as for
214 M1.
215 To evaluate the effect of the CNC incorporation method on the film properties, pure
216 thermoplastic starch films were additionally prepared, plasticised with 30% of glycerol
217 respect to starch, containing or not 1 wt% of CNC in the films incorporated by methods
218 1 and 2 (samples S-CNC-M1 and S-CNC-M2). The compatibilised starch-PLA blend
219 films with 1 wt% of CNC were also prepared by methods 1 and 2 (samples
220 S(PCL_{5G})PLA_{20}-CNC-M1 and S(PCL_{5G})PLA_{20}-CNC-M2).
221
222 *2.5. Characterisation of the films*
223 2.5.1. *Field emission scanning electron microscopy (FESEM) and X-Ray diffraction*
224 *pattern*

225 Microstructural analyses of the cross-section of the films were carried out in a Field
226 Emission Scanning Electron Microscope (FESEM Ultra 55, Zeiss, Oxford Instruments,
227 U.K). Samples were conditioned in desiccators with P_2O_5 for 2 weeks at 25°C, and
228 afterwards adequately put on support stubs and coated with platinum. Observations
229 were carried out at 1.5 kV.
230 An X-Ray diffraction analysis of the different samples was performed using a
231 diffractometer (XRD, Bruker AXS/D8 Advance) at 40 kV and 40 mA. Scattered
232 radiation was detected in an angular range 2θ: 5-30° with a step size of 0.05º. The
233 degree of crystallinity (Xc) of the samples, expressed as a percentage, was calculated,
234 using OriginPro 8.5 software, from the ratio of crystalline peak areas and the integrated
235 area of XRD diffractograms, assuming Gaussian profiles for crystalline and amorphous
236 peaks (Collazo-Bigliardi et al., 2018b; Ortega-Toro et al., 2016b).
237
238 2.5.2. *Thermal behaviour*
239 A thermogravimetric analyser (TGA 1 Star^e System analyser, Mettler-Toledo, Inc.,
240 Switzerland) was used to study the thermal stability of the samples. The measurements
241 of the thermal weight loss were taken over a temperature range of 25 to 600 ºC at
242 20ºC/min, under nitrogen atmosphere (gas flow: 10 mL min^{-1}). The initial degradation
243 temperature (T_{Onset}) and peak temperature (T_{Peak}) were obtained using the STAR^e
244 Evaluation Software (Mettler-Toledo, Inc., Switzerland), from the first derivative of the
245 resulting weight loss curves.
246 The phase transitions in the polymer matrices were evaluated by means of Differential
247 Scanning Calorimetry (DSC 1 Star^e System, Mettler-Toledo Inc., Switzerland). Film
248 samples of 7-9 mg were placed into aluminium pans and sealed. The thermograms were
249 obtained in a heating cycle from 25 ºC to 160 ºC at 10 ºC/min, cooled until 25 ºC, and

250 then heated in a second cycle under the same conditions. In the first scan, the bonded
251 water in the film was eliminated, and in the second heating scan, the glass transition of
252 starch and PLA was analysed.
253
254 2.5.3. *Mechanical properties*
255 The mechanical performance of the samples was analysed following the ASTM
256 standard method D882 (ASTM, 2001). A universal test machine (TA.XTplus model,
257 Stable Micro Systems, Haslemere, England) was used to obtain the stress-strain curves.
258 From these curves, the elastic modulus (EM), tensile strength at break point (TS) and
259 the elongation at break (ε) of the films were determined. The film thickness was taken
260 into account for the calculations. Conditioned (25 ºC, 53% RH) samples of 25 x 100
261 mm were mounted in the film-extension grips of the testing machine and stretched at 50
262 mm/min until break. Ten replicates were made for each formulation.
263
264 2.5.4. *Moisture content, water vapour permeability (WVP) and oxygen permeability*
265 *(OP)*
266 The samples conditioned at 53% RH were dried in a natural convection oven (J.P.
267 Selecta, S.A. Barcelona, Spain) for 24 h at 60 °C to determine the equilibrium moisture
268 content of the films. Then, they were placed in a desiccator at 25 ºC with P_2O_5 for a
269 week to adjust the relative humidity to close to 0%. The moisture content of the samples
270 was calculated by varying the weight between the wet sample (53% RH) and the dry
271 sample (0% RH).
272 The water vapour permeability (WVP) of the films was determined following the
273 gravimetric method, E96-95 (ASTM, 1995; McHugh, Avena-Bustillos, & Krochta,
274 1993), with some modifications. Payne permeability cups (Elcometer SPRL, Hermelle/s

275 Argenteau, Belgium), 3.5 cm in diameter, were used with 5 mL of bidistilled water and
276 the adjusted film. Each cup was placed into a desiccator equilibrated with $Mg(NO_3)_2$
277 saturated solution (53% HR, 25 °C) and inserted into a chamber at 25 ºC. The cups were
278 weighed periodically (± 0.0001 g) until the steady state was reached. The WVP was
279 calculated from the slope of the curves of weight loss versus time as reported by Ortega-
280 Toro et al. (2016a).
281 The oxygen permeability of the films (50 cm^2 film area) was determined using OX-
282 TRAN equipment, Model 2/21 ML (Mocon Lippke, Neuwied, Germany) in samples
283 conditioned at 25 ºC and 53% RH. Film thickness was considered in all cases in order to
284 obtain the OP values. The oxygen transmission values were evaluated every 10 min
285 until equilibrium.
286
287 2.5.5. *Optical properties*
288 The film transparency was measured through the internal transmittance (Ti), applying
289 the Kubelka-Munk theory of multiple scattering (Hutchings, 1999), using the film
290 reflection spectra obtained on both black and white backgrounds, as described by Talón
291 et al. (2017). Reflection spectra from 400 to 700 nm were obtained by using a spectro-
292 colorimeter CM- 3600d (Minolta Co., Tokyo, Japan).
293
294 *2.6. Antioxidant performance of the films on sunflower oil*
295 To evaluate the antioxidant properties of the S-PLA compatibilised films with
296 antioxidant extract, their potential positive effect on the retardation of sunflower oil
297 oxidation was analysed. To this end, the method described by Galarza, Haas, de
298 Oliveira, & Hickmann (2017) was used. Film samples (area of 7.5 cm × 4 cm) were
299 thermosealed to form bags using a vacuum packing machine (SAECO Vacio Press

300 Elite, Barcelona, Spain). 5 mL of commercial sunflower oil were placed into each bag
301 and thermo-sealed. How effective the films were at delaying sunflower oil oxidation
302 was evaluated in comparison to S-PLA compatibilised blend films without antioxidant
303 extract. As the control sample, an open glass Petri dish containing 5 mL of sunflower oil
304 was considered. All of the samples were stored at 30 ºC and 53% RH and exposed to
305 fluorescent light at an intensity of 1000-1500 lux (measured using a digital Luxometer;
306 model RS Pro ILM1332A, RS Components, Madrid, Spain). The oxidative stability of
307 sunflower oil was measured in terms of peroxide index after 5, 9, 14, 19 and 23 days of
308 storage. For that purpose, a titrimetric method was employed (IUPAC, 1987), using an
309 automatic titrator (Titrando, Metrohm Ion Analysis, Switzerland). 1 g of oil was
310 dissolved in 10 mL of solvent (glacial acetic acid:1-decanol at 3:2 volume ratio,
311 containing 10-15 $mg \cdot L^{-1}$ of iodine) and mixed with 200 µL of saturated KI solution and
312 kept in the dark for 1 min. Then, 50 mL of distilled water was added, and the solution
313 was titrated with 0.01 M or 0.001 M Na_2S2O_3, depending on the expected peroxide
314 index. A blank control sample (without sunflower oil) was prepared by the same
315 procedure.
316
317 *2.7. Statistical analysis*
318 Statgraphics Centurion XVI software (Manugistics Corp., Rockville, Md.) was used to
319 perform the statistical analyses of the results by means of analysis of variance
320 (ANOVA). Fisher's least significant difference (LSD) procedure was used at the 95%
321 confidence level.
322
323 **3. Results and discussion**

3.1. Effect of the CNC on the film functional properties as affected by the incorporation method

The incorporation method of CNC from their aqueous dispersion into the polymeric matrices is critical since water content must be reduced in the internal mixer to prevent overpressure during the polymer melt blending or polymer hydrolysis. The CNC dispersion could be dried before the incorporation process and drying methods that are effective at maintaining the inherent nano-scale dimensions, such as freeze drying, spray drying or supercritical drying, have been described (Ng et al., 2015). Nevertheless, CNC are aggregated in the dry form and re-dispersion in the polymer melt represents a challenge, on top of the difficulty involved in handling them in dry form (Brinchi et al., 2013). In this work, two different methods were used to transfer CNC to the polymer blend: their previous transference to the glycerol used as plasticizer (M1) and the previous thermoprocessing of the starch phase suspended in the initial CNC dispersion in an open two-roll mill, which favours water evaporation while the starch gelatinization occurs (M2). In this sense, 1 wt% of CNC was incorporated into both S-PLA compatibilised blends and net TPS films, for comparison purposes. Tables 2 and 3 include the tensile properties (elastic modulus: EM, tensile strength: TS and elongation at break: ε), thickness, barrier properties (water vapour permeability: WVP and oxygen permeability: OP) and moisture content of the obtained films.

Significant differences in tensile properties were obtained for films with the same composition obtained by using both methods for the CNC transference. Using M1, reductions in the EM of the films, with respect to that of the corresponding film without CNC, of about 42 and 33%, respectively for starch and starch-PLA blend, was obtained. However, a significant increase in EM was detected when CNC were directly incorporated into the starch phase in the open two-roll mill (132 and 148%, respectively

for the starch and starch-PLA blend). A similar effect was observed on the TS, while the film extensibility was only notably reduced when using M2 for CNC incorporation. This indicates the different reinforcing effect of CNC on the matrix depending on the transference method. The greater improvement in the film resistance and stiffness when CNC were directly incorporated into the starch phase from the water dispersion points to the strong interfacial interaction between crystalline cellulose and starch during the melt blending through the great surface area of the CNC (Collazo-Bigliardi et al., 2017b). In contrast, the previous transference of the CNC to the glycerol could lead to the formation of glycerol-CNC complexes through hydroxyl hydrogen bonds. CNC-glycerol interactions would favour the glycerol carbon exposure on the outside of the molecular complex, giving particles with a more hydrophobic surface and lower ability to disperse in the hydrophilic starch continuous phase of the film, where their reinforcing capacity would be more appreciable. Dispersion of the more hydrophobic CNC-glycerol particles in the starch phase would contribute to a reduction in the cohesion forces of the matrix, thus reducing the films' stiffness and resistance to break. In the S-PLA blend, the CNC-glycerol complexes would exhibit more affinity with the less-polar molecules of PLA than with the continuous polar starch phase and so, the glycerol-CNC particles could be better dispersed in the PLA domains, which, in turn, are dispersed in the starch matrix. Fig.1 shows the FESEM micrograph of compatibilised blend films, where the good interfacial adhesion between the dispersed PLA domains and continuous starch phase may be observed, as well as the reduced size of the PLA domains, as discussed in previous studies (Collazo-Bigliardi et al., 2019b)

Fig.1 also shows the FESEM micrographs of the compatibilised blend films with CNC transferred by both methods, where no CNC aggregates could be observed at the used magnification level, while qualitative differences may be appreciated at the PLA-starch

374 interface. M2 led to lower interfacial adhesion of the polymers than M1. This could be
375 due to the different location of CNC, which can also contribute to the interfacial
376 interactions, depending on their prevalent distribution in each phase and their
377 association, or not, with the glycerol molecules. In the S-PLA blend, the CNC-glycerol
378 particles dispersed within the PLA domains could improve the interfacial affinity of
379 both polymers.
380 Kargarzadeh, Johar, & Ahmad (2017) also observed an increase in EM (up to 70%) and
381 TS (up to 52%) with the addition of 6% of CNC from rice husk to cassava starch films
382 obtained by casting. Savadekar & Mhaske (2012) also incorporated CNC from cotton
383 fibres into thermoplastic starch blends at 0.4 wt% with good reinforcement efficiency.
384 The formation of a percolation network favours the enhancement of the film mechanical
385 properties because of the interaction among the CNC by intra- and inter-molecular
386 hydrogen bonds and/or the mutual entanglement between the CNC and the starch
387 matrix. Moreover, the intrinsic stiffness of crystalline cellulose, associated with the
388 crystalline structure, could also contribute to the increase in EM. This fact was also
389 reported by Sung, Chang, & Han (2017) for PLA matrices obtained by extrusion
390 process when freeze-dried CNC from coffee silverskin were incorporated. Authors also
391 reported that the stiffening effect of the filler led to significant local stress
392 concentrations and reduced strain to failure. Karkarzadeh et al. (2017) and Sung et al.
393 (2017) indicated that the main factors determining the reinforcing effect of nano-scale
394 fillers are the good dispersion and adhesion between the filler and the polymer matrix,
395 which, in turn, are affected by the CNC load in the blend (Dhar, Tarafder, Kumar, &
396 Katiyar, 2016).
397 Barrier properties were also affected by the CNC incorporation method. In starch films,
398 WVP was reduced by 28 and 36% when CNC were incorporated by methods 1 and 2,

399 respectively. In contrast, OP was only significantly reduced (by 40%) when using M2.
400 Reduction in WVP was also reported by Fabra, López-Rubio, Ambrosio-Martín, &
401 Lagaron (2016) for thermoplastic corn starch films with different contents of bacterial
402 cellulose nanowhiskers. The different effect of the CNC on barrier properties,
403 depending on the transference method, agrees with the different film microstructure and
404 the prevalent location of the CNC in each case.
405 In starch-PLA compatibilised films, WVP was only reduced (by 28%) by method 2,
406 whereas OP increased by 30% by method 1 and decreased by 42 % by method 2. These
407 different effects are coherent with the more hydrophobic nature of the CNC particles
408 when transferred from the glycerol and their prevalent location in the dispersed PLA
409 domains, whereas CNC incorporated into the starch phase (method 2) provided a more
410 efficient barrier capacity, similar to that observed in the net starch films.
411 The role of CNC at improving barrier properties is mainly related with their crystalline
412 structure, which hinders the diffusion of molecules (O_2, CO_2, H_2O) through the
413 biopolymer matrix. The formation of hydrogen-bonded structures and a percolation
414 network promotes the tortuosity factor of the matrix (Collazo-Bigliardi et al., 2018b;
415 Luzi et al., 2016), which mainly depends on the matrix-filler adhesion, degree of
416 dispersion, aspect ratio of filler and polymer chain immobilization (Sung et al., 2017).
417 In polymer blends with phase separation, the percolation network in the continuous
418 phase will be more effective than that in the dispersed domains, which also points to the
419 different distribution of CNC (in the continuous or dispersed phase), according to the
420 incorporation method.
421 As regards crystallization, Fig. 2 shows X-ray diffraction pattern and degree of
422 crystallinity (Xc) of the different samples containing CNC incorporated by the two
423 methods. The main characteristic crystalline peaks of starch were detected in all

samples at 2θ values of around 12.9º and 19.8º, which are associated with the crystalline structure of amylose type V (Castillo et al., 2013; Ortega-Toro, Contreras, Talens, & Chiralt, 2015), although some peaks associated with A form (2θ: 18-18.5º) could also be observed. The characteristic peak of crystalline PLA on 2θ of 17º (Muller et al., 2017b) was not observed, coherent with its amorphous nature. Likewise, no peaks of crystalline PCL (2θ: 21.6º, 22.2º and 23.3º; Ortega-Toro et al., 2016b) were detected for the grafted PCL, either because of its low concentration in the blend or its crystallization inhibition by the anchoring of the polar groups (Ortega-Toro et al., 2016b). Cellulosic micro- or nano-fillers exhibited typical crystalline peaks of type I cellulose at 2θ: 17º and 21.4º (Collazo-Bigliardi et al., 2018b) but they were not observed, probably due to their low content in the film. The incorporation of CNC directly into the starch phase (method 2) slightly promoted the amylose crystallization in starch films, which could be due to the favoured interaction of amylose and crystalline cellulose, which can act as nucleating agents, as reported by other authors (Ferreira et al., 2018). However, this effect was not observed in the starch-PLA blend.

Fig. 3 shows TGA and derivate (DTGA) curves obtained for the studied formulations. TGA curves exhibited several degradation phases of differing intensities for every sample; the first phase can be attributed to the bonded water evaporation and the degradation of low molecular weight components and, afterwards, the partially overlapped thermal degradation of the polymers, starch, PLA and PCL_G, and the cellulosic fraction, took place. These different phases are reflected in the DTGA curves as peaks or shoulders. The shoulder in the main peak at about 380 ºC would mainly correspond to the degradation of the grafted PCL with higher degradation temperatures (341-381 ºC, Ortega-Toro et al., 2016b), partially overlapped with the final degradation of PLA. The comparison of samples containing CNC incorporated by both methods and

449 control sample (free of lignocellulosic fractions) reflects differences in the peak and
450 shoulder temperatures in both the first and the main peak. No differences were found
451 between control sample and that processed by method 1, but samples processed by
452 method 2 exhibited a lower temperature for the first peak and a higher temperature for
453 the main peak, with temperature displacements for the shoulders. This can be attributed
454 to the different interactions of CNC with the polymers in both cases, resulting in
455 changes in the degradation behaviour of the different blend components (Kargarzadeh et
456 al., 2018). Table 4 also shows the glass transition temperature (Tg) of S and PLA in the
457 different blend films. This is an important parameter since it indicates the maximum
458 temperature of use of the packaging material before its softening (Ortega-Toro et al.,
459 2017). The addition of CNC by method 1 or 2 did not significantly affect the values of
460 Tg of any of the polymers, although a slight tendency to increase was observed. Other
461 authors (Chen, Zhou, Zou, & Gao, 2019; Ilyas, Sapuan, Ishak, & Zainudin, 2018)
462 reported an increase in the Tg values of starch nanocomposites with CNC obtained by
463 casting. However the increase in the CNC content implied a reduction in the water
464 content of the films that, in turn, reduced its plasticization effect. Glass transition
465 temperature in the studied films were obtained in completely dried films (conditioned in
466 P_2O_5) where no water plasticization effect was expected and no significant effect of
467 CNC was detected on the Tg values. However, hydrogen bonds between hydroxyl
468 groups of crystalline cellulose and starch chains can be assumed, as reported by other
469 authors (Kargarzadeh et al., 2018; Karimi, Abdulkhani, Tahir, & Dufresne, 2016)
470 favouring the compatibility of CNC in the starch matrix.
471 As concerns transparency (Fig. 4), the control sample (free of lignocellulosic fractions)
472 exhibited relatively low transparency that can be attributed to the dispersion of the PLA
473 domains in the starch matrix, as observed in the FESEM images, which implies an

474 increase in the dispersive component of light. The incorporation of CNC into the blend
475 slightly modified film transparency, depending on the incorporation method. This
476 agrees with the microstructural observations that reflect differences in the component
477 arrangement mainly at interfacial level, which may affect the light dispersion pattern
478 and so, the film transparency, as reported by Muller et al. (2017b).
479
480 *3.2. Effect of cellulosic fibres on the film's functional properties*
481 The microstructural impact of cellulosic fibres from coffee husk on the S-PLA
482 compatibilised matrix can be observed in Fig. 1, where the FESEM micrographs of the
483 film cross-section are shown. The CF could be clearly seen embedded in the film matrix
484 with good interfacial adhesion. However, CF provoked a weakening effect on the film
485 matrix reflected in the fact that the EM values were lower than in the control film,
486 although they did not provoke significant changes in the film resistance to break and
487 extensibility. Likewise, the barrier properties of the films were negatively affected by
488 CF; no significant changes in the WVP were observed, but OP increased by 40% with
489 respect to the control film.
490 The addition of CF did not provoke notable changes in the film transparency, polymer
491 crystallization pattern or in the degree of crystallinity; neither did it influence the
492 thermal behaviour of the blend in terms of the thermodegradation of components or the
493 polymer glass transition. Then, CF behaved as a quasi-inert filler that, at the used ratio,
494 did not improve film properties. However, CF incorporated at 1% in net starch films
495 increased their elastic module by 50% with respect to the control film, with no changes
496 in barrier properties (Collazo-Bigliardi et al., 2018a). The lack of effect brought about
497 by CF in the compatibilised starch-PLA blend could be explained by the starch film that
498 is already reinforced by the dispersed PLA that makes the fibre effect less appreciable.

Likewise, in terms of barrier properties, fibres do not seem to lead to a notable increase in the tortuosity of the path to permeation of the water and gas molecules, with respect to that promoted by the PLA dispersed in the starch matrix, and the expected improvement in the film barrier capacity was not observed.

3.3. Effect of antioxidant extract on the film's functional properties

The incorporation of the active extract into the blend films led to morphological changes in both the continuous starch phase and the PLA dispersed phase, as compared with the control sample, as shown in Fig. 1. In fact, the ability of the extract compounds to interact with the starch matrix, contributing to the formation of a more compact and homogeneous matrix, has previously been reported in other studies (Collazo-Bigliardi et al., in press; Talón et al., 2017). Likewise, PLA in the dispersed phase could also interact with these compounds. The acid nature of phenolic acids could even partially hydrolyse the polyester chains. Caffeic and chlorogenic acids were the main phenolic compounds present in coffee husk, and vanillic, gallic, tannic and protocatechuic acids were also found in small quantities (Aguiar, Estevinho, & Santos, 2016).

The tensile properties of the blend films were not significantly affected by the presence of the antioxidant extract, despite the fact that this had a great reinforcement effect in net starch films. This suggests that compounds could interact better with the dispersed PLA than with the starch, which dilutes the potential reinforcing effects in the film's continuous phase. As concerns barrier properties, no significant effect was observed on the WVP, but the OP was reduced by 15% respect to that of the control film. OP reduction brought about by the extract incorporation was also observed in net starch films, which was attributed to the oxygen scavenging capacity of the compounds in line with their antioxidant capacity (Collazo-Bigliardi et al., in press).

524 The incorporation of the extract did not modify the crystallization pattern of the films,
525 but slightly reduced the degree of crystallinity in line with its amorphous nature. The
526 thermodegradation behaviour was also slightly modified by the extract, due to the
527 presence of low molecular compounds which degrade at low temperature. Likewise, the
528 Tg of starch and PLA changed with respect to the control film, thus indicating the
529 interactions of the extract compounds with both polymers. The Tg value of starch
530 increased, as previously observed for net starch films containing this extract (Collazo-
531 Bigliardi et al., in press) and the Tg of PLA decreased, according to a plasticizing effect
532 of the compounds in this polymer phase or to the possible partial de-polymerization of
533 PLA provoked by phenolic acids, as previously mentioned.
534 The films containing active extract exhibited the lowest transparency level which is
535 mainly caused by the selective light absorption of the extract compounds, mainly at low
536 wavelengths. This could be considered positive because of the potential protection
537 capacity of the films for use in food applications, reducing the light-induced oxidation
538 reactions (Collazo-Bigliardi et al., 2018c).
539 The antioxidant capacity of these films was evaluated through their ability to preserve
540 sunflower oil from oxidation. The antioxidant capacity of this film formulation was
541 compared to that of the control film and to an open oil sample. The PV values reflect
542 the initial oxidation stage of oil since it is related with the presence of peroxides derived
543 from the polyunsaturated fatty acids existing in the sample (Galarza et al., 2017).
544 Hydroperoxides are produced as primary oxidation products that could be derived into
545 secondary products. The progress of the PV in the different samples throughout 23 days
546 is shown in Fig. 5. The PV of sunflower oil in the initial stage was 2.2 mEq O_2/kg, as
547 also reported by other authors (Kiralan et al., 2017; Mohdaly, Sarhan, Mahmoud,
548 Ramadan, & Smetanska, 2010). A remarkable increase in this value was found for the

549 open control sample (135 mEq O_2/kg in the final stage). However, the samples with and
550 without antioxidant compound were kept below the required limits, even for the control
551 film, at the end of the experiment (~5 mEq O_2/kg). The Codex Alimentarius established
552 a limit of PV in 10 mEq O_2/kg for refined oils (Codex-Alimentarius, 1999). This
553 behaviour is attributable to the great oxygen barrier capacity of the films, mainly made
554 up of starch. The lowest PV were obtained in the sample packaged in the film with AE,
555 wherein the presence of the antioxidant compounds from coffee husk prevented the
556 oxidation of sunflower oil. Similar results were described by Reis, de Souza, da Silva,
557 Martins, Nunes, & Druzian (2015) analysing the incorporation of mango pulp and yerba
558 mate extract into cassava starch films, which were effective at preserving palm oil.
559 Galarza et al. (2017) also reported a good preservation of sunflower oil oxidation when
560 packaged in bags formed with glycerol-plasticised films from rice flour (RRF) and red
561 rice starch (RRS) in a 9:1 RRF:RRS ratio.
562
563 **4. Conclusions**
564 Lignocellulosic fractions of coffee husk could be used to improve the functional
565 properties of compatibilised starch PLA films, depending on their final use. Of the
566 cellulosic fractions, CF was not adequate to enhance the functionality of the blend film,
567 but CNC previously incorporated into the starch phase were effective at reinforcing the
568 tensile properties of the material (148% and 45% increases in EM and TS, respectively)
569 and at reducing the WVP and OP of the films (28% and 42 % reductions, respectively in
570 WVP and OP). Likewise, the antioxidant extract did not impart a better mechanical
571 performance to the blend films, but reduced their oxygen permeability and conferred
572 antioxidant capacity, promoting their usefulness for the purposes of preventing food
573 oxidation reactions.

Acknowledgements

The authors thank the Ministerio de Economía y Competitividad (Spain) for the financial support provided through Project AGL2016-76699-R. The authors also wish to thank the Electron Microscopy Service of the UPV for their technical assistance.

References

Aguiar, J., Estevinho, B. N., & Santos, L. (2016). Microencapsulation of natural antioxidants for food application - The specific case of coffee antioxidants - A review. *Trends in Food Science & Technology, 58*, 21-39.

Alves, R. C., Rodrigues, F., Nunes, M. A., Vinha, A. F., & Oliveira, M. B. P. P. (2017). State of the art in coffee processing by-products. In C. M. Galanakis (Ed.), *Handbook of coffee processing by-products* (pp. 1–26). Cambridge: Academic Press.

ASTM. (1995). Standard test methods for water vapor transmission of materials. Standard Designations: E96-95. In Annual books of ASTM (pp. 406-413). Philadelphia, PA: American Society for Testing and Materials.

ASTM (2001). Standard test method for tensile properties of thin plastic sheeting. Standard Designations: D882. Annual book of ASTM standards. Philadelphia, PA: American Society for Testing and Materials.

Azeredo, H., Rosa, M. F., & Mattoso, L. H. (2017). Nanocellulose in bio-based food packaging applications. *Industrial Crops and Products*, *97*, 664-671.

Balaji, A. B., Pakalapati, H., Khalid, M., Walvekar, R., & Siddiqui, H. (2017). Natural and synthetic biocompatible and biodegradable polymers. In N. Gopal Shimpi

(Ed.), *Biodegradable and biocompatible polymer composites* (pp. 3-32). United Kingdom: Woodhead Publishing.

Berthet, M. A., Angellier-Coussy, H., Machado, D., Hilliou, L., Stabler, A., Vicente, A., & Gontard, N. (2015). Exploring the potentialities of using lignocellulosic fibres derived from three food by-products as constituents of biocomposites for food packaging. *Industrial Crops and Products*, *69*, 110-122.

Brigham, C. (2018). Biopolymers: Biodegradable alternatives to traditional plastics. In B. Török, & T. Dransfield (Eds.), *Green chemistry* (pp. 753-770). Amsterdam: Elsevier Inc.

Brinchi, L., Cotana, F., Fortunati, E., & Kenny, J. M. (2013). Production of nanocrystalline cellulose from lignocellulosic biomass: Technology and applications. *Carbohydrate Polymers*, *94*, 154–169.

Castillo, L., López, O., López, C., Zaritzky, N., García, M. A., Barbosa, S., & Villar, M. (2013). Thermoplastic starch films reinforced with talc nanoparticles. *Carbohydrate Polymers*, *95(2),* 664-674.

Chen, Q., Zhou, L., Zou, J., & Gao, C. (2019). The preparation and characterization of nanocomposite film reinforced by modified cellulose nanocrystals. International *Journal of Biological Macromolecules, 132*, 1155-1162.

Codex-Alimentarius. (1999). Codex-Standards for fats and oils from vegetable sources (Vol. 210, p. 1).

Collazo-Bigliardi, S., Ortega-Toro, R., & Chiralt, A. (2018a). Properties of Micro- and nano-reinforced biopolymers for food applications. In T. Gutiérrez (Ed.), *Polymers for food applications* (pp. 61-99). Springer.

621 Collazo-Bigliardi, S., Ortega-Toro, R., & Chiralt, A. (2018b). Isolation and
622 characterisation of microcrystalline cellulose and cellulose nanocrystals from coffee
623 husk and comparative study with rice husk. *Carbohydrate Polymers*, *191*, 205-215.
624 Collazo-Bigliardi, S., Ortega-Toro, R., & Chiralt, A. (2018c). Reinforcement of
625 thermoplastic starch films with cellulose fibres obtained from rice and coffee husks.
626 *Journal of Renewable Materials*, *6*, 599-610.
627 Collazo-Bigliardi, S., Ortega-Toro, R., & Chiralt, A. (2019a). Using grafted poly(ε-
628 caprolactone) for the compatibilization of starch-polylactic acid blends. *Reactive
629 and Functional Polymers, 142*, 25-35.
630 Collazo-Bigliardi, S., Ortega-Toro, R., & Chiralt, A. (2019b). Improving properties of
631 thermoplastic starch films by incorporating active extracts and cellulose fibres
632 isolated from rice or coffee husk. *Food Packaging and Shelf Life, 22*, 100383.
633 Cong-Cong, X., Bing, W., Yi-Qiong, P., Jian-Sheng, T., & Tong, Z. (2017). Advances
634 in extraction and analysis of phenolic compounds from plant materials. *Chinese
635 Journal of Natural Medicines*, *15(10),* 721-731.
636 Dhar, P., Tarafder, D., Kumar, A., & Katiyar, V. (2016). Thermally recyclable
637 polylactic acid/cellulose nanocrystal films through reactive extrusion process.
638 *Polymer*, *87*, 268-282.
639 Dorris, A., & Gray, D. G. (2012). Gelation of cellulose nanocrystals suspensions in
640 glycerol. *Cellulose, 19*, 687-694.
641 Fabra, M. J., López-Rubio, A., Ambrosio-Martín, J., & Lagaron, J. M. (2016).
642 Improving the barrier properties of thermoplastic corn starch-based films containing
643 bacterial cellulose nanowhiskers by means of PHA electrospun coatings of interest
644 in food packaging. *Food Hydrocolloids*, *61*, 261-268.

645 Ferreira, F. V., Dufresne, A., Pinheiro, I. F., Souza, D. H. S., Gouveia, R. F., Mei, L. H.
646 I., & Lona, L. M. F. (2018). How do cellulose nanocrystals affect the overall
647 properties of biodegradable polymer nanocomposites: A comprehensive review.
648 *European Polymer Journal*, *108*, 274-285.
649 Galarza, C., Costa, T. M. H., de Oliveira Rios, A., & Flôres, S. H. (2017). Comparative
650 study on the properties of films based on red rice (Oryza glaberrima) flour and
651 starch. *Food Hydrocolloids*, *65*, 96-106.
652 Hamad, K., Kaseem, M., Ayyoob, M., Joo, J., & Deri, F. (2018). Polylactic acid
653 blends: The future of green, light and tough. *Progress in Polymer Science*, *85*, 83-
654 127.
655 Hutchings, J. B. (1999). Food color and appearance (2nd ed.). Gaithersburg, Maryland,
656 USA: Aspen Publishers, Inc.
657 Ilyas, R. A., Sapuan, S. M., Ishak, M. R., & Zainudin, E. S. (2018). Development and
658 characterization of sugar palm nanocrystalline cellulose reinforced sugar palm starch
659 bionanocomposites. *Carbohydrate Polymers, 202*, 186-202.
660 IUPAC (International Union of Pure and Applied Chemistry). (1987). Standard method
661 for the analysis of oils, fats and derivatives; Paquot, C., Hautfenne, A. London, U.K:
662 Blackwell Scientific Publications.
663 Kargarzadeh, H., Johar, N., & Ahmad, I. (2017). Starch biocomposite film reinforced
664 by multiscale rice husk fiber. *Composite Science and Technology*, *15*, 147–155.
665 Kargarzadeh, H., Huang, J., Lin, N., Ahmad, I., Mariano, M., Dufresne, A., Thomas,
666 S., & Galeski, A. (2018). Recent developments in nanocellulose-based
667 biodegradable polymers, thermoplastic polymers, and porous nanocomposites.
668 *Progress in Polymer Science*, *87*, 197-227.

669 Karimi, S., Abdulkhani, A., Tahir, P. M., & Dufresne, A (2016). Effect of cellulosic
670 fiber scale on linear and non-linear mechanicalperformance of starch-based
671 composites. *International Journal of Biological Macromolecules, 91*, 1040-1044.
672 Kiralan, M., Ulaş, M., Özaydin, A., Özdemır, N., Özkan, G., Bayrak, A., & Ramadan,
673 M. F. (2017). Blends of cold pressed black cumin oil and sunflower oil with
674 improved stability: a study based on changes in the levels of volatiles, tocopherols
675 and thymoquinone during accelerated oxidation conditions. *Journal of Food*
676 *Biochemistry*, 41(1), e12272.
677 Koch, K. (2018). Starch-based film. In M. Sjöö & L. Nilsson (Eds), *Starch in food* (pp.
678 747-767). Woodhead Publishing.
679 Laurienzo, P., Malinconico, M., Mattia, G., & Romano, G. (2006). Synthesis and
680 characterization of functionalized crosslinkable poly(ε-caprolactone).
681 *Macromolecular Chemistry and Physics*, *207*, 1861-1869.
682 Luzi, F., Fortunati, E., Jiménez, A., Puglia, D., Pezzolla, D., Gigliotti, G., Kenny, J.
683 M., Chiralt, A., & Torre, L. (2016). Production and characterization of PLA_PBS
684 biodegradable blends reinforced with nanocrystals extracted from hemp fibres.
685 *Industrial Crops and Products*, *93*, 276–289.
686 McHugh, T. H., Avena-Bustillos, R., & Krochta, J. M. (1993). Hydrophobic edible
687 films: Modified procedure for water vapour permeability and explanation of
688 thickness effects. *Journal of Food Science*, *58(4),* 899-903.
689 Mohdaly, A. A. A., Sarhan, M. A., Mahmoud, A., Ramadan, M. F., & Smetanska, I.
690 (2010). Antioxidant efficacy of potato peels and sugar beet pulp extracts in
691 vegetable oils protection. *Food chemistry*, *123(4),* 1019-1026.

692 Müller, P., Bere, J., Fekete, R., Móczó, J., Nagy, B., Kállay, M., Gyarmati, B., &
693 Pukánszky, B. (2016). Interactions, structure and properties in PLA/plasticized
694 starch blends. *Polymer*, *103*, 9-18.
695 Muller, J., González-Martínez, C., & Chiralt, A. (2017a). Combination of poly(lactic)
696 acid and starch for biodegradable food packaging. *Materials*, *10*, 952.
697 Muller, J., González-Martínez, C., & Chiralt, A. (2017b). Poly(lactic) acid (PLA) and
698 starch bilayer films, containing cinnamaldehyde, obtained by compression
699 moulding. *European Polymer Journal*, *95*, 56-70.
700 Murariu, M., & Dubois, P. (2016). PLA composites: From production to properties.
701 *Advanced drug delivery reviews*, *107*, 17-46.
702 Ng, H. M., Sin, L. T., Tee, T. T., Bee, S. T., Hui, D., Low, C. Y., et al. (2015).
703 Extraction of cellulose nanocrystals from plant sources for application as
704 reinforcing agent in polymers. *Composites Part B Engineering, 75*, 176–200.
705 Ogunsona, E., Ojogbo, E., & Mekonnen, T. (2018). Advanced material applications of
706 starch and its derivatives. *European Polymer Journal*, *108*, 570-581.
707 Ortega-Toro, R., Contreras, J., Talens, P., & Chiralt, A. (2015). Physical and structural
708 properties and thermal behaviour of starch-poly(e-caprolactone) blend films for
709 food packaging. *Food Packaging and Shelf Life, 5*, 10-20.
710 Ortega-Toro, R., Collazo-Bigliardi, S., Talens, P., & Chiralt, A. (2016a). Influence of
711 citric acid on the properties and stability of starch-polycaprolactone based films.
712 *Journal of Applied Polymer Science*, *42220*, 1-16.
713 Ortega-Toro, R., Santagata, G., Gomez d'Ayala, G., Cerruti, P., Talens, P., Chiralt, A.,
714 & Malinconico, M. (2016b). Enhancement of interfacial adhesion between starch
715 and grafted poly(ε-caprolactone). *Carbohydrate Polymers*, *147*, 16-27.

716 Ortega-Toro, R., Bonilla, J., Talens, P., & Chiralt, A. (2017). Starch-based materials in
717 food packaging. In M. A. Villar, S. E. Barbosa, M. A. García, L. A. Castillo, & O.
718 V. López (Eds.), *Future of starch-based materials in food packaging* (pp. 257-312).
719 Aspen Publishers.
720 Patel, J. P., & Parsania, P. H. (2018). Characterization, testing, and reinforcing materials
721 of biodegradable composites. In N. G. Shimpi (Ed.), *Biodegradable and*
722 *biocompatible polymer composites* (pp. 55–79). United Kingdom: Woodhead
723 Publishing.
724 Piñeros-Castro, Y., & Otálvaro, A. M. (2014). Use of lignocellulosic biomass, some
725 research in Colombia. In Y. Piñeros-Castro, & J. Melo (Eds.), Antioxidant activity
726 in liquids from pre-treatments with hot water carried out on rice husk (pp. 237-254).
727 Bogotá. ISBN: 978-958-725-152-4.
728 Reis, L., De Souza, C., Da Silva, J., Martins, A., Nunes, I., & Druzian, J. (2015). Active
729 biocomposites of cassava starch: The effect of yerba mate extract and mango pulp as
730 antioxidant additives on the properties and the stability of a packaged product. *Food*
731 *and Bioproducts Processing*, *94*, 382-391.
732 Requena, R., Vargas, M., & Chiralt, A. (2018). Obtaining antimicrobial bilayer starch
733 and polyester-blend films with carvacrol. *Food Hydrocolloids, 83*, 118-133.
734 Savadekar, N. M., & Mhaske, S. T. (2012). Synthesis of nano cellulose fibers and effect
735 on thermoplastics starch based films. *Carbohydrate Polymers*, *89*, 146–151.
736 Shavandi, A., Bekhit, A. E. A., Saeedi, P., Izadifar, Z., Bekhit, A. A., &
737 Khademhosseini, A. (2018). Polyphenol uses in biomaterials engineering.
738 *Biomaterials*, *167*, 91-106.

739 Sung, S. H., Chang, Y., & Han, J. (2017). Development of polylactic acid
740 nanocomposite films reinforced with cellulose nanocrystals derived from coffee
741 silverskin. *Carbohydrate Polymers*, *169*, 495-503.
742 Talón, E., Trifkovic, K. T., Nedovic, V. A., Bugarski, B. M., Vargas, M., Chiralt, A., &
743 González-Martínez, C. (2017). Antioxidant edible films based on chitosan and
744 starch containing polyphenols from thyme extracts. *Carbohydrate Polymers*, *157*,
745 1153-1161.
746 Tampau, A., González-Martínez, C., & Chiralt, A. (2018). Release kinetics and
747 antimicrobial properties of carvacrol encapsulated in electrospun poly-(ε-
748 caprolactone) nanofibres. Application in starch multilayer films. *Food*
749 *Hydrocolloids, 79*, 158-169.
750

Figure captions

Fig. 1. FESEM micrographs of the cross-section of pure thermoplastic starch (S) and compatibilised S-PLA blends containing or not CNC incorporated by different methods (M1: glycerol transference, M2: direct thermoprocessing in two-roll mill), cellulose fibres (CF) and active extracts (AE) from coffee husk.

Fig. 2. X-ray diffraction patterns and crystallinity degree (Xc, %) of pure thermoplastic starch (S) and compatibilised S-PLA blends containing or not CNC incorporated by different methods (M1: glycerol transference, M2: direct thermoprocessing in two roll mill), cellulose fibres (CF) and active extracts (AE) from coffee husk.

Fig. 3. TGA and DTGA curves of compatibilised S-PLA blends containing or not CNC incorporated by different methods (M1: glycerol transference, M2: direct thermoprocessing in two roll mill), cellulose fibres (CF) and active extracts (AE) from coffee husk.

Fig. 4. Internal transmittance (Ti) spectra of compatibilised S-PLA blends containing or not CNC incorporated by different methods (M1: glycerol transference, M2: direct thermoprocessing in two roll mill), cellulose fibres (CF) and active extracts (AE) from coffee husk. Embedded table shows the Ti values at 460 nm.

Fig. 5. Peroxide Index (mEq O_2/kg), B) of sunflower oil packaged in films of compatibilised S-PLA blends containing or not antioxidant extract (AE), compared with the control open samples.

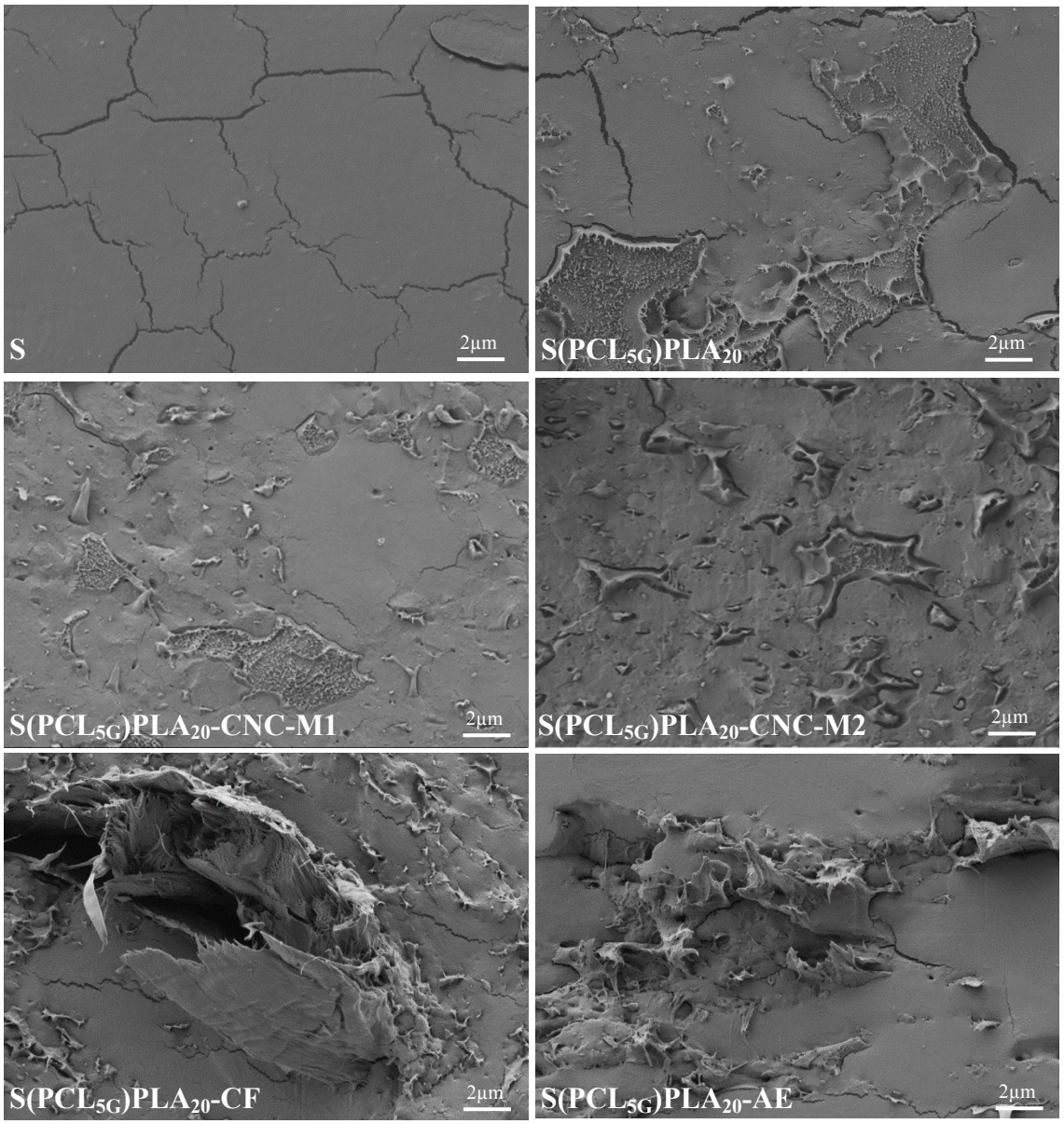
S
2μm
S(PCL5G)PLA20
2μm
S(PCL5G)PLA20-CNC-M1
2μm
S(PCL5G)PLA20-CNC-M2
2μm
S(PCL5G)PLA20-CF
2μm
S(PCL5G)PLA20-AE
2μm

Fig. 1.

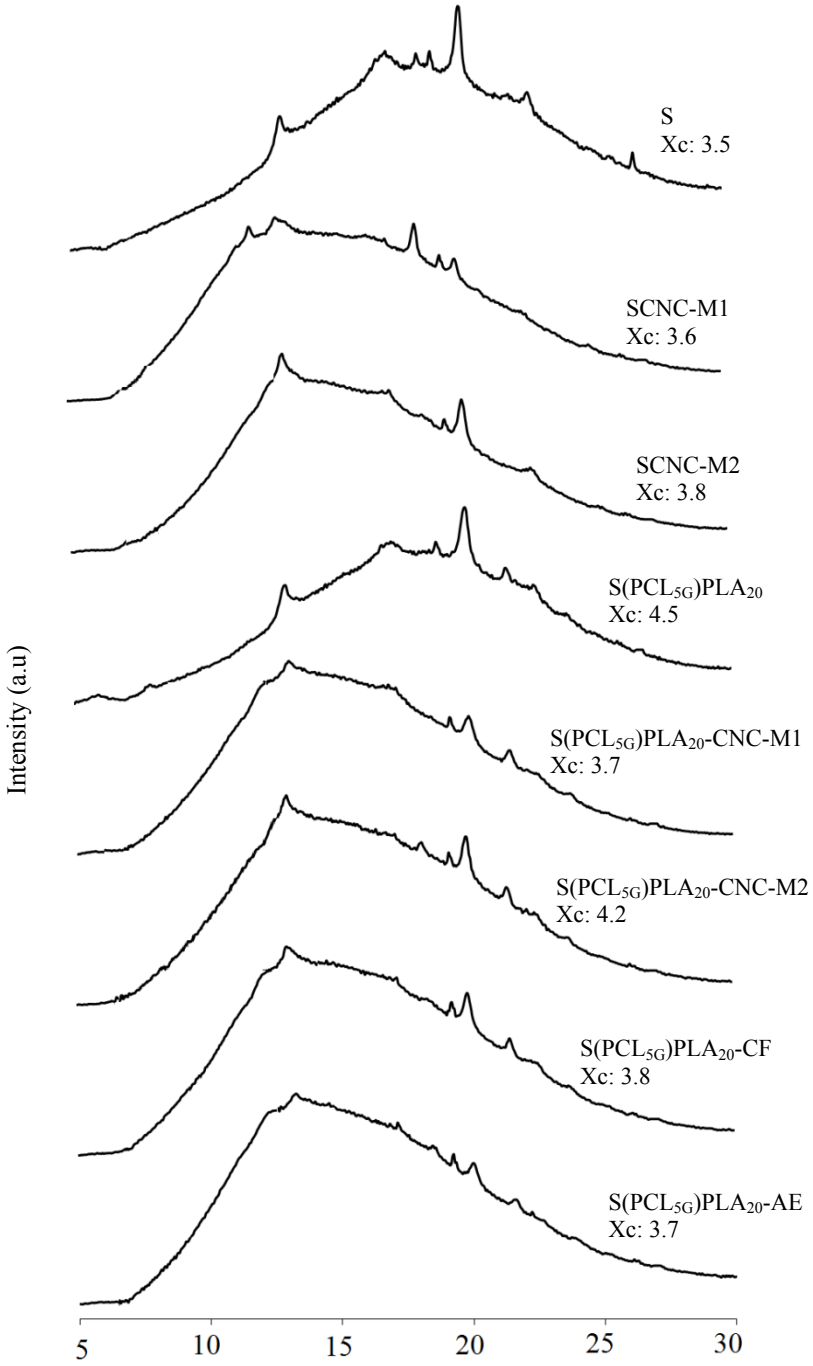
S
Xc: 3.5
SCNC-M1
Xc: 3.6
SCNC-M2
Xc: 3.8
S(PCL5G)PLA20
Xc: 4.5
S(PCL5G)PLA20-CNC-M1
Xc: 3.7
S(PCL5G)PLA20-CNC-M2
Xc: 4.2
S(PCL5G)PLA20-CF
Xc: 3.8
S(PCL5G)PLA20-AE
Xc: 3.7
Intensity (a.u)
5
10
15
20
25
30
2□ (Degrees)

Fig. 2.

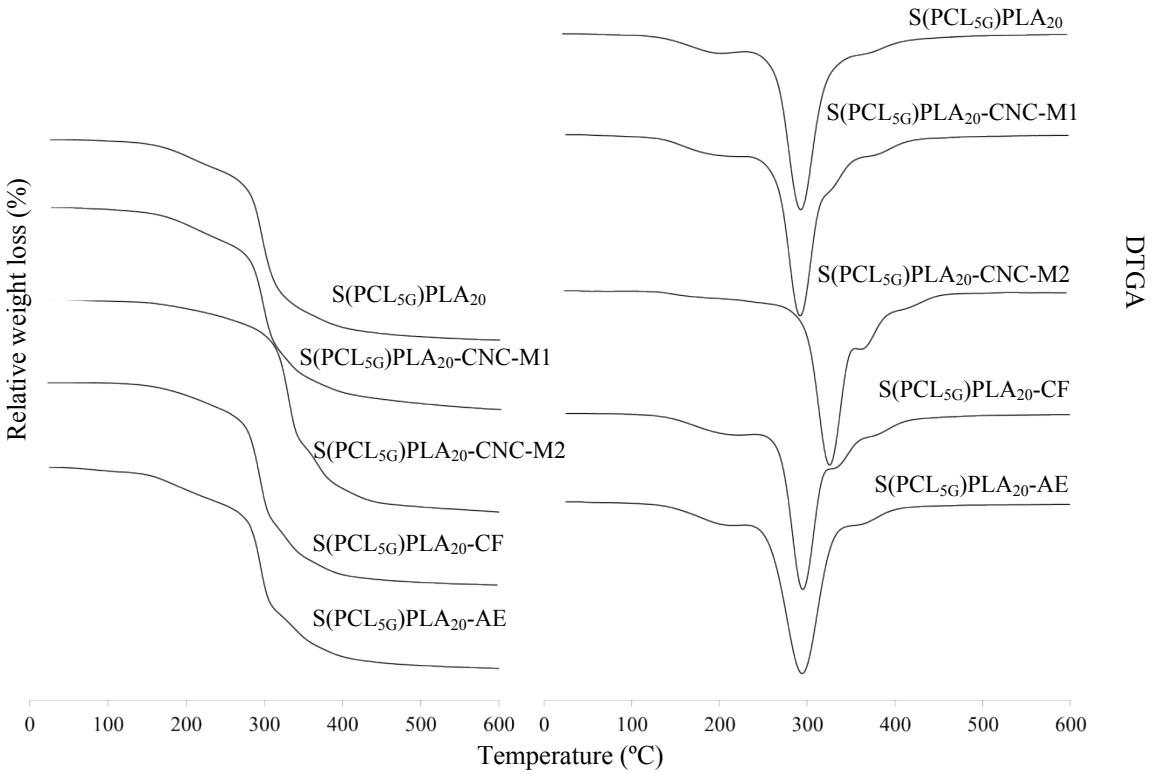
Relative weight loss (%)
S(PCL5G)PLA20
S(PCL5G)PLA20-CNC-M1
S(PCL5G)PLA20-CNC-M2
S(PCL5G)PLA20-CF
S(PCL5G)PLA20-AE
0
100
200
300
400
500
600
Temperature (ºC)
DTGA

Fig. 3.

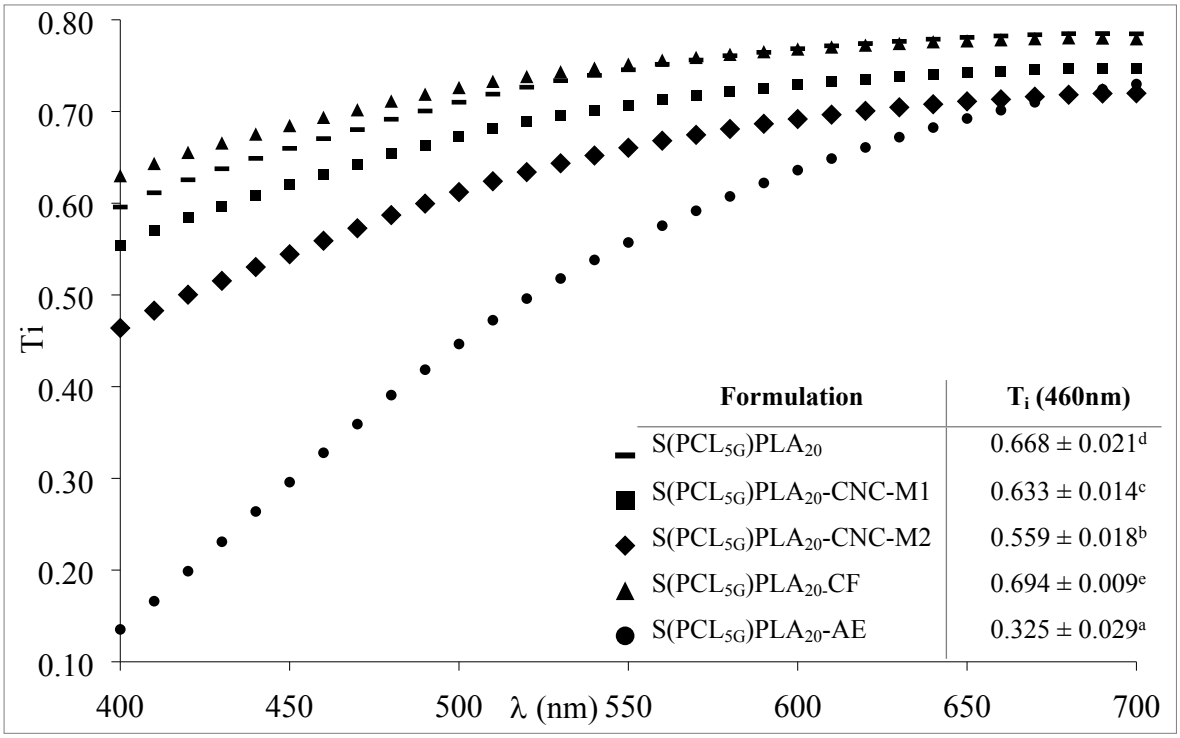
0.80
0.70
0.60
0.50
0.40
0.30
0.20
0.10
Ti
400
450
500
λ (nm)
550
600
650
700
Formulation
T_i (460nm)
S(PCL5G)PLA20
0.668 ± 0.021d
S(PCL5G)PLA20-CNC-M1
0.633 ± 0.014c
S(PCL5G)PLA20-CNC-M2
0.559 ± 0.018b
S(PCL5G)PLA20.CF
0.694 ± 0.009e
S(PCL5G)PLA20-AE
0.325 ± 0.029a

Fig. 4

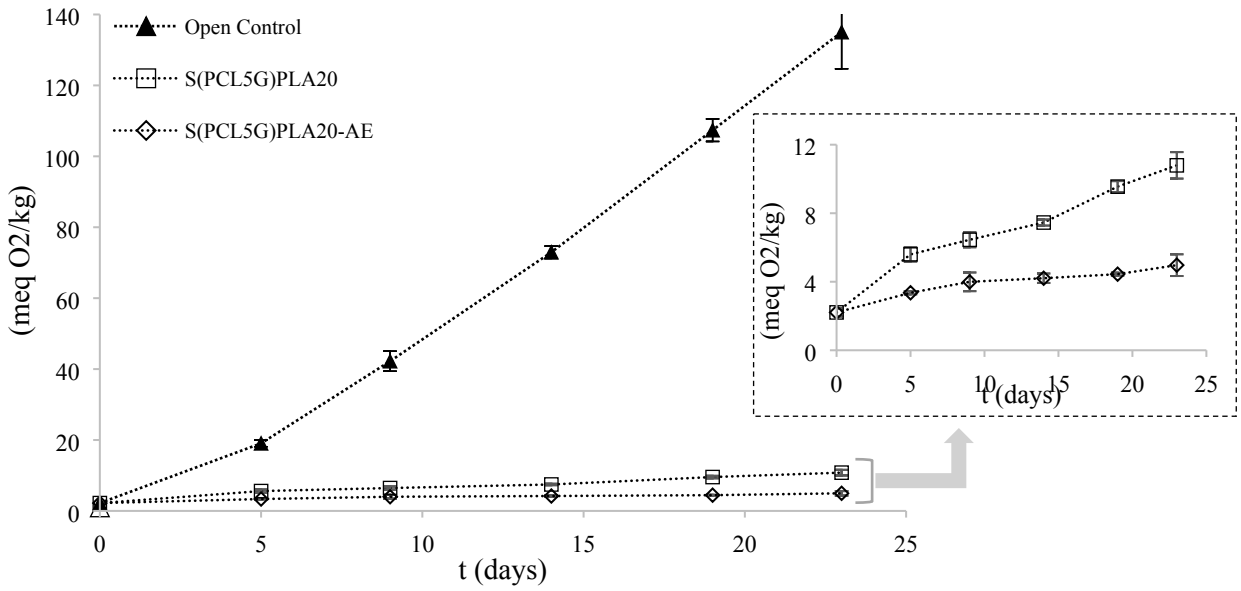
Open Control
S(PCL5G)PLA20
S(PCL5G)PLA20-AE
(meq O2/kg)
t (days)
0
20
40
60
80
100
120
140
0
5
10
15
20
25
(meq O2/kg)
t (days)
0
4
8
12
0
5
10
15
20
25

Fig. 5

Table 1. Mass fraction (Xi, g compound/g dried film) of the different components: Starch (S), glycerol (Gly), glycidyl methacrylate grafted polycaprolactone (PCL_G), polylactic acid (PLA), cellulose nanocrystals (CNC) from coffee husk, cellulose fibres from coffee husk (CF) and antioxidant extract from coffee husk (AE).

Formulations	X_S	X_{Gly}	X_{PCLg}	X_{PLA}	$X_{CNC/CF}$	X_{AE}
$S(PCL_{5G})PLA_{20}$	0.6410	0.1923	0.0385	0.1282	-	-
$S(PCL_{5G})PLA_{20}$-CNC	0.6346	0.1904	0.0381	0.1269	0.0100	-
$S(PCL_{5G})PLA_{20}$ -CF	0.6346	0.1904	0.0381	0.1269	0.0100	-
$S(PCL_{5G})PLA_{20}$ -AE	0.6410	0.1346	0.0385	0.1282	-	0.0577

Table 2. Tensile properties (EM: elastic modulus, TS: tensile strength, ε: elongation at break point) of pure thermoplastic starch (S) and containing CNC incorporated by different methods (M1: glycerol transference, M2: direct thermoprocessing in two roll mill), compatibilised S-PLA blends containing CNC incorporated by M1 and M2, cellulose fibres (CF) and active extracts (AE) from coffee husk (films conditioned at 53% RH and 25 ºC).

Formulation	EM (MPa)	TS (MPa)	ε (%)	Thickness (mm)
S	77 ± 15^{b}	5.2 ± 1.6^{b}	64.9 ± 0.5^{f}	0.20 ± 0.02^{bc}
S-CNC-M1	45 ± 3^{a}	3.8 ± 0.2^{a}	55.3 ± 1.4^{e}	0.20 ± 0.02^{b}
S-CNC-M2	179 ± 4^{d}	6.6 ± 0.4^{c}	35.1 ± 4.7^{d}	0.20 ± 0.01^{bc}
S(PCL$_{5G}$)PLA$_{20}$	195 ± 35^{d}	7.6 ± 0.3^{de}	21.1 ± 1.9^{b}	0.19 ± 0.01^{ab}
S(PCL$_{5G}$)PLA$_{20}$-CNC-M1	140 ± 16^{c}	8.0 ± 0.5^{e}	28.3 ± 3.9^{c}	0.20 ± 0.02^{b}
S(PCL$_{5G}$)PLA$_{20}$-CNC-M2	515 ± 29^{g}	11.0 ± 0.3^{f}	12.6 ± 2.0^{a}	0.21 ± 0.01^{c}
S(PCL$_{5G}$)PLA$_{20}$-CF	132 ± 15^{c}	7.0 ± 0.3^{cd}	20.5 ± 1.4^{b}	0.18 ± 0.01^{a}
S(PCL$_{5G}$)PLA$_{20}$-AE	183 ± 13^{d}	6.9 ± 0.9^{cd}	19.8 ± 2.3^{b}	0.18 ± 0.01^{a}

Different superscript letters within the same row indicate significant differences among formulations ($p<0.05$).

Table 3. Mean values and standard deviation of barrier properties (water vapor permeability: WVP, oxygen permeability: OP) and moisture content of pure thermoplastic starch (S) containing or not CNC incorporated by different methods (M1: glycerol transference, M2: direct thermoprocessing in two roll mill) and compatibilised S-PLA blends containing CNC incorporated by M1 and M2, cellulose fibres (CF) and active extracts (AE) from coffee husk (films conditioned at 53% RH and 25 ºC).

Formulation	Moisture content (g water/g dried film)	WVP ($g \cdot mm \cdot kPa^{-1} \cdot h^{-1} \cdot m^{-2}$)	OP x10^{14} ($cm^3 \cdot m^{-1} \cdot s^{-1} \cdot Pa^{-1}$)
S	0.096 ± 0.007^{c}	14.9 ± 0.4^{d}	10.3 ± 0.1^{b}
S-CNC-M1	0.098 ± 0.005^{c}	10.7 ± 0.6^{c}	11.8 ± 0.9^{c}
S-CNC-M2	0.097 ± 0.006^{c}	9.3 ± 1.3^{bc}	6.2 ± 0.8^{a}
S(PCL_{5G})PLA_{20}	0.065 ± 0.004^{a}	10.1 ± 0.4^{bc}	19.9 ± 0.6^{e}
S(PCL_{5G})PLA_{20}-CNC-M1	0.091 ± 0.006^{bc}	10.8 ± 1.2^{c}	25.9 ± 0.7^{f}
S(PCL_{5G})PLA_{20}-CNC-M2	0.092 ± 0.005^{bc}	7.3 ± 0.9^{a}	11.6 ± 0.8^{bc}
S(PCL_{5G})PLA_{20}-CF	0.104 ± 0.003^{d}	8.9 ± 1.0^{ab}	28.1 ± 0.4^{g}
S(PCL_{5G})PLA_{20}-AE	0.086 ± 0.001^{b}	8.4 ± 0.9^{ab}	17.2 ± 0.2^{d}

Different superscript letters within the same row indicate significant differences among formulations ($p < 0.05$).

Table 4. Mean values and standard deviation of onset and peak temperatures for thermal degradation and glass transition temperature (Tg; second heating scan on DSC) of S-PLA films with cellulosic material and antioxidant extracts from coffee husk, conditioned in P_2O_5.

Samples	[138-205]ºC		[250-400]ºC			Second heating scan	
	Onset (ºC)	Peak (ºC)	Onset (ºC)	Peak (ºC)	Endset (ºC)	Tg (ºC) Starch	Tg (ºC) PLA
S(PCL$_{5G}$)PLA$_{20}$	146 ± 4^{a}	195 ± 2^{bc}	269 ± 1^{b}	296 ± 1^{a}	392 ± 2^{a}	106 ± 1^{a}	49.3 ± 0.7^{b}
S(PCL$_{5G}$)PLA$_{20}$-CNC-M1	141 ± 3^{a}	193 ± 8^{b}	268 ± 1^{b}	294 ± 2^{a}	400 ± 0.3^{b}	107 ± 2^{a}	48.2 ± 0.9^{ab}
S(PCL$_{5G}$)PLA$_{20}$-CNC-M2	145 ± 2^{a}	171 ± 0.2^{a}	305 ± 0.2^{c}	329 ± 1^{b}	438 ± 4^{c}	107 ± 2^{a}	48.3 ± 0.9^{ab}
S(PCL$_{5G}$)PLA$_{20}$-CF	151 ± 5^{ab}	204 ± 0.5^{c}	270 ± 1^{b}	296 ± 0.2^{a}	400 ± 2^{b}	108 ± 1^{a}	49.5 ± 0.6^{b}
S(PCL$_{5G}$)PLA$_{20}$-AE	156 ± 3^{b}	200 ± 0.1^{bc}	258 ± 0.2^{a}	295 ± 1^{a}	404 ± 2^{b}	110 ± 1^{b}	47.7 ± 0.3^{a}

Different superscript letters within the same column indicate significant differences between formulations ($p < 0.05$).